iScience

CellPress
OPEN ACCESS

Article

Identifying shared transcriptional risk patterns between atherosclerosis and cancer

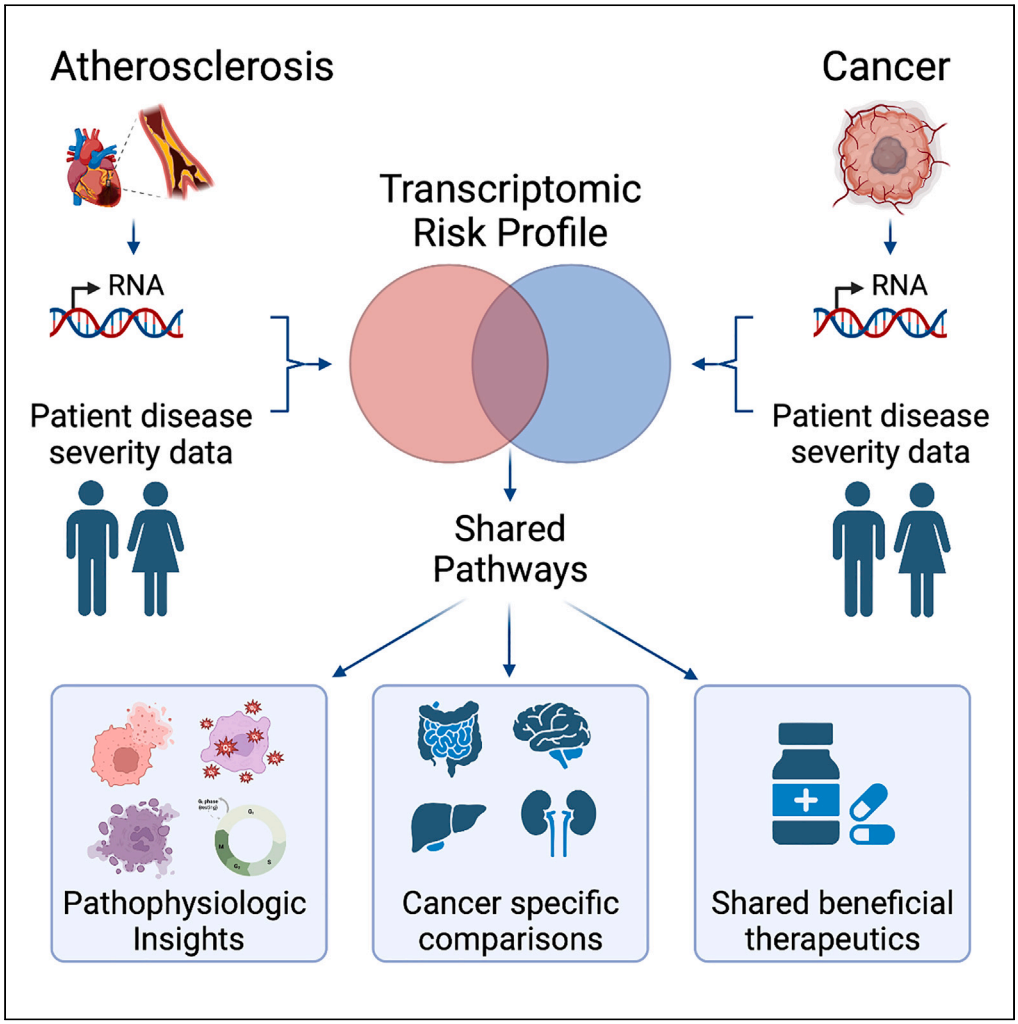

Richard A. Baylis, Hua Gao, Fudi Wang, Caitlin F. Bell, Lingfeng Luo, Johan L.M. Björkegren, Nicholas J. Leeper

nleeper@stanford.edu

Highlights

Cancer and atherosclerosis have long been thought to share pathologic similarities

These were quantified using gene expression correlated with disease indices

Numerous known and novel dysregulated processes were found to be common

These were used to predict compounds potentially capable of treating both diseases

Baylis et al., iScience 26, 107513
September 15, 2023
https://doi.org/10.1016/j.isci.2023.107513

iScience

CellPress
OPEN ACCESS

Article

Identifying shared transcriptional risk patterns between atherosclerosis and cancer

Richard A. Baylis,[1,2,3,4,8] Hua Gao,[1,2,8] Fudi Wang,[1,2] Caitlin F. Bell,[1,7] Lingfeng Luo,[1,2] Johan L.M. Björkegren,[5,6] and Nicholas J. Leeper[1,2,7,9,10,*]

SUMMARY

Cancer and cardiovascular disease (CVD) are the leading causes of death worldwide. Numerous overlapping pathophysiologic mechanisms have been hypothesized to drive the development of both diseases. Further investigation of these common pathways could allow for the identification of mutually detrimental processes and therapeutic targeting to derive mutual benefit. In this study, we intersect transcriptomic datasets correlated with disease severity or patient outcomes for both cancer and atherosclerotic CVD. These analyses confirmed numerous pathways known to underlie both diseases, such as inflammation and hypoxia, but also identified several novel shared pathways. We used these to explore common translational targets by applying the drug prediction software, OCTAD, to identify compounds that simultaneously reverse the gene expression signature for both diseases. These analyses suggest that certain tumor-specific therapeutic approaches may be implemented so that they avoid cardiovascular consequences, and in some cases may even be used to simultaneously target co-prevalent cancer and atherosclerosis.

INTRODUCTION

Cancer and the complications of atherosclerotic cardiovascular disease (CVD) make up nearly half of all deaths in the US. Despite knowing a great deal about each of these diseases individually, surprisingly little is known about how these diseases interact within patients or the common dysregulated genes and pathways that these diseases share. It has long been recognized that patients with either cancer or CVD share numerous risk factors.[1] Consequently, these diseases often occur in the same patient population and many times occur simultaneously in the same patients. Further, preclinical studies have demonstrated that both diseases can be driven through similar processes. For example, surgical occlusion of coronary arteries in mice exacerbates atherosclerosis formation,[2] and recently has been shown to exacerbate breast cancer resulting in larger, more metastatic tumors.[3] In a similar manner, hyperlipidemia, the primary stimulus to induce atherogenesis in mice, has been shown to intensify tumor growth in mice injected with several different tumor cell lines.[4] One explanation for the shared risk factors and pathogenic drivers is the numerous shared dysregulated processes that are known to contribute to the pathogenesis of both diseases.

There are now multiple clinical studies demonstrating mutual benefit when shared pathogenic pathways are targeted. For example, the CANTOS trial tested a neutralizing IL1β antibody in high-risk patients and found not only a significant reduction in major adverse cardiovascular events, but also a reduction in cancer mortality, which was driven by a benefit in lung cancer.[5,6] However, several dedicated cancer trials have thus far failed to show similar benefits, which may be due to differences in patient characteristics and cancer stage.[7] A recent study from our lab demonstrated for the first time in humans that inhibiting CD47, a 'don't eat me' signal known to be an effective target for multiple cancers, also had a significant beneficial impact on vascular inflammation.[8] Immune checkpoint inhibitors, which have rapidly revolutionized the treatment of numerous cancers,[9] provide additional clinical rationale for comparative studies of atherosclerosis and cancer. Indeed, the profound benefits that ICIs have had on the management of cancer have been somewhat offset by a significant increase in CVD which appears to be driven in part by exacerbating atherosclerosis.[10–12] Taken together, these data support careful identification and targeting of shared pathogenic features of both diseases.

[1]Department of Surgery, Division of Vascular Surgery, Stanford University School of Medicine, Stanford, CA, USA

[2]Stanford Cardiovascular Institute, Stanford, CA, USA

[3]Department of Medicine, Division of Cardiology, University of California, San Francisco, CA, USA

[4]Department of Medicine, Massachusetts General Hospital, Boston, MA, USA

[5]Department of Medicine, Karolinska Institute, Huddinge, Sweden

[6]Department of Genetics and Genomic Sciences, Institute of Genomics and Multiscale Biology, Icahn School of Medicine at Mount Sinai, New York, NY, USA

[7]Department of Medicine, Division of Cardiovascular Medicine, Stanford University School of Medicine, Stanford, CA, USA

[8]These authors contributed equally

[9]Senior author

[10]Lead contact

*Correspondence: nleeper@stanford.edu

https://doi.org/10.1016/j.isci.2023.107513

To date, studies investigating the interface between cancer and atherosclerosis have come from the field of cardio-oncology where, motivated by the increased cardiovascular risk among cancer patients, the cardiotoxic effects of cancer therapeutics have been characterized and managed. However, this has resulted in a largely reactionary approach to managing cardiovascular risk in cancer patients and have not included efforts to proactively manage co-prevalent disease. In this study, we take an innovative strategy to compare the pathogenic pathways of atherosclerosis and numerous common cancer subtypes, to identify key shared processes that could be targeted to derive mutual benefit. We then leverage the drug prediction software, OCTAD, to identify compounds that target these pathways.

RESULTS

Leveraging transcriptomic data to characterize genes and pathways associated with cancer and atherosclerotic CVD severity

To better understand shared disease mechanisms between atherosclerosis and cancer, we used transcriptomic data that could be correlated with patient outcomes or disease severity (Figure 1A). For The Cancer Genome Atlas (TCGA) data, tumor gene expression has been correlated with patient survival. To interrogate atherosclerotic CVD in a similar manner, we primarily used data from STARNET,[13] which has accumulated RNA-seq data from the atherosclerotic aortic root taken from ~600 patients during coronary artery bypass grafting. Transcriptomic data from the atherosclerotic aortic wall were correlated with two angiographic parameters that describe disease severity including the DUKE CAD severity score[14] and the angiographic CAD SYNTAX score.[15] To compare healthy versus diseased tissue, we compared RNA-seq data derived from the non-atherosclerotic mammary artery with that patient's atherosclerotic aortic root. As a validation dataset, we incorporated the publicly available data from the Biobank of Karolinska Endarterectomy (BiKE) data, which had performed transcriptomic analyses on carotid plaques from 126 patients and then monitored for subsequent ischemic events (MI or stroke).[16] At 44 months follow up, 25 patients had experienced an ischemic event and were termed symptomatic while the remaining 101 patients remained asymptomatic. We performed Cox regression to correlate the transcriptomic information with disease severity/survival. For simplicity, we have referred to the correlation of transcriptomic and disease information as the "transcriptional risk profile".

Comparison of transcriptional risk profile for atherosclerotic CVD and all TCGA cancer subtypes reveals several important pathogenic commonalities including metabolism, stemness, and EMT

To understand the shared pathways that mediate risk for both diseases, we performed Hallmark pathway enrichment on the transcriptional risk profiles for cancer and atherosclerosis and plotted the results on opposing axes such that mutually detrimental pathways occupied quadrant 1, while those in quadrant 3 would be mutually beneficial. Quadrants 2 and 4 would highlight pathways that have the opposite effect on the diseases (e.g., worse for CVD but better for cancer; see schematic in Figure 1B).

When all cancers and atherosclerotic CVD were analyzed together, several consistent trends emerged including increased risk with increased glycolysis and reduced oxidative phosphorylation and fatty acid metabolism, which is consistent with the Warburg effect in cancer and has recently been suggested as a marker of high-risk atherosclerotic plaques (Figure 1B).[17] Interestingly, quadrant 1 was also dominated by pathways mediating cellular stemness including WNT, Notch, and Hedgehog signaling and cellular polarity including apical surface and junction, suggesting that an increased stem-like signature is mutually detrimental in both diseases. Finally, epithelial-to-mesenchymal transitions (EMT) and TGFβ signaling, the key regulator of EMT, were found to be mutually detrimental. This process is known to play a critical role in tumor metastasis, however in atherosclerosis TGFβ has traditionally been viewed as a plaque stabilizing pathway by increasing collagen deposition by vascular smooth muscle in the fibrous cap. Interestingly, a process which is genetically similar to EMT, endothelial to mesenchymal transition (EndoMT), has recently been shown to correlate with reduced atherosclerotic plaque stability in humans,[18,19] suggesting that TGFβ can have protective or detrimental effects depending on the stage of the lesions and cellular respondents.[20] The fact that our prediction shows an overall detrimental impact of TGFβ signaling may suggest that the stage of lesion development from patients in STARNET and BiKE may have had pathogenic EndoMT as the predominate effect of TGFβ signaling. However, this remains an active area of research that will require additional inquiry.

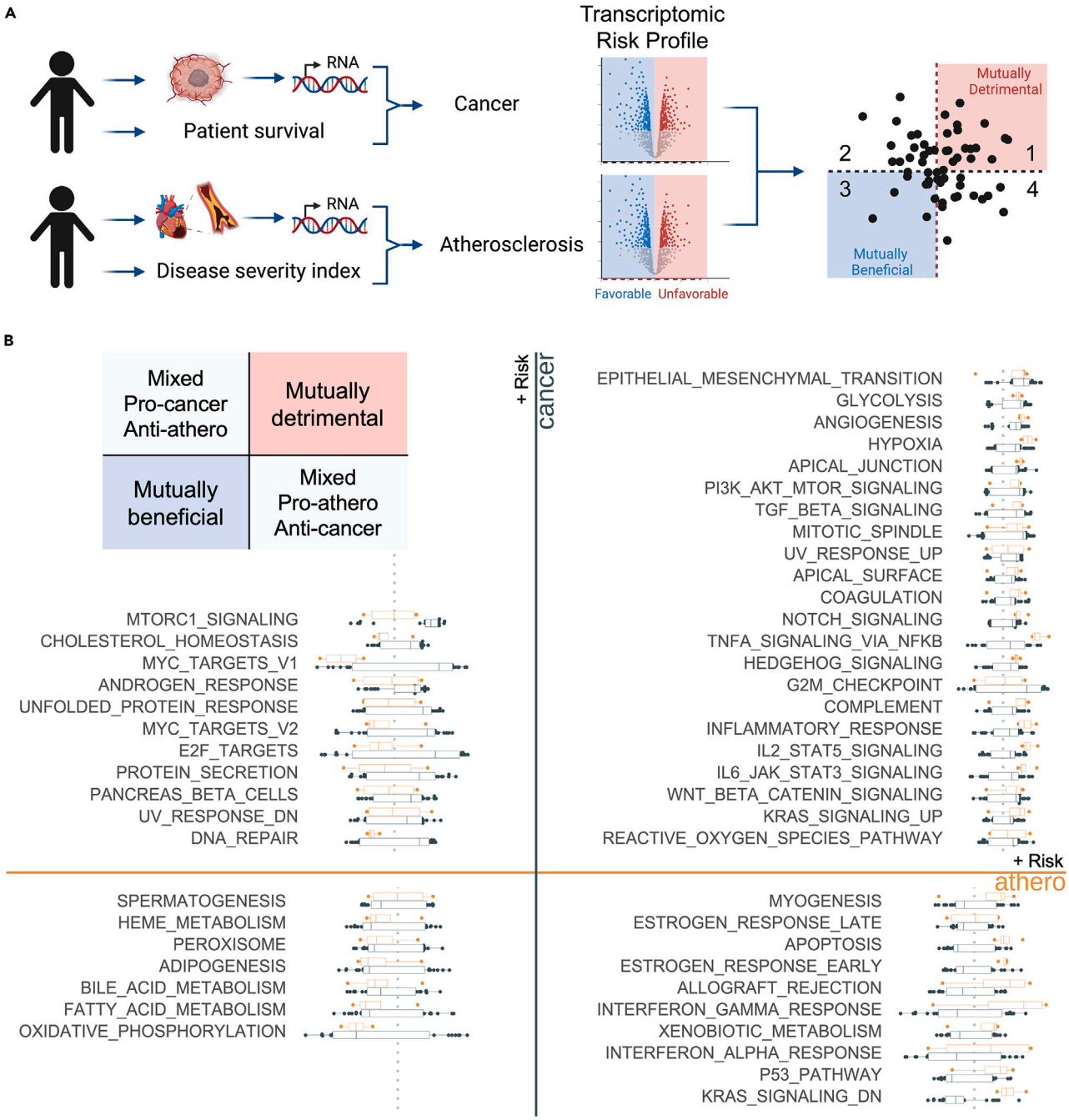

Figure 1. Comparison of transcriptional risk profile for atherosclerosis and all TCGA cancer subtypes

(A) Schematic describing the generation of transcriptomic risk profiles for atherosclerosis and cancer, which were then plotted on opposing axes to reveal shared biology.

(B) Hallmark pathway analysis with disease severity for atherosclerosis (X axis) and cancer (Y axis). Importantly, both diseases were exacerbated by a glycolytically skewed metabolism and improved by a metabolism enriched for oxidative phosphorylation and fatty acid utilization. Numerous pathways that regulate cellular plasticity and differentiation were mutually detrimental for cancer and atherosclerosis. Finally, epithelial to mesenchymal transitions and its key regulatory pathway, TGFβ signaling, were also mutually detrimental. The box plot overlaid on the scatter dots represents the IQR (interquartile range) with whiskers that extend 1.5 times the IQR from the box edges.

Clustering transcriptional risk profiles based on pathway enrichment reveals that certain cancers are more transcriptionally similar to atherosclerotic CVD

To assist in visualizing the data, we plotted Hallmark pathway enrichment for the transcriptional risk profile of each of the datasets using a heatmap (Figure 2A) and the dimensionality reduction algorithm, UMAP (Figure 2B; abbreviations for each cancer can be found in Figure S1).[21] Reassuringly, this revealed tight clustering of the atherosclerosis datasets (i.e., STARNET and BiKE). We hypothesized that the transcriptional risk profiles of cancer and atherosclerotic CVD would be largely distinct and result in clear separation between cancer and atherosclerosis datasets. However, contrary to our hypothesis, we observed that cancer and atherosclerosis could not be distinguished based on their transcriptional risk profiles. Certain cancers clustered tightly with the CAD datasets while others clustered more distantly, which we refer to as athero-similar and athero-dissimilar cancers, respectively (Figure 2B). Interestingly, there were no obvious features distinguishing the two groups of cancers (e.g., cell type of origin, tissue type, smoking association). To determine if differences in the abundance of immune cell populations drove the transcriptional differences between the two groups of cancers, the Gene Set Cancer Analysis (GSCA) immune cell tool was applied to the cancer datasets. The abundance of each individual immune cell population predicted by GSCA was then averaged and compared between the athero-similar and dissimilar cancers. Although variation in immune cell abundance was apparent when individual cancers were compared, there was no significant difference in the abundance of individual immune cell populations between the athero-similar and -dissimilar cancers (Figures S2A and B). These data suggest that the differences between athero-similar and -dissimilar cancers are not simply driven by differences in immune cell recruitment.

Pro-atherogenic inflammatory pathways are detrimental in athero-similar cancers but beneficial in athero-dissimilar cancers

Next, the athero-similar and -dissimilar cancers were analyzed separately to see which pathways were divergent between them (individual pathways highlighted in Figure 2C; full plots in Figure S3). When athero-similar cancers were plotted against the atherosclerotic CVD datasets, many of the mutually detrimental pathways were inflammatory or immunomodulatory. For example, multiple cytokine signaling pathways including IL2, IL6, IFNγ, and TNFα were observed as well the general inflammatory response pathway. The complement pathway was also differentially enriched, components of which have recently been shown to promote atherosclerosis. Specifically, C3 expression by clonally proliferating SMC has been shown to worsen atherosclerosis by desensitizing them to phagocytic clearence.[22] The role for complement in cancer has been studied extensively and, interestingly, C3 knockout mice are largely protected from orthotopic tumor formation.[23] In stark contrast, these same inflammatory pathways appear to have a protective role in the athero-dissimilar cancers, an observation that may have important clinical relevance. To see if differences in the role of these immune pathways corresponded to differential susceptibilities to immune checkpoint inhibitors (ICIs), we tabulated FDA approvals for each of the ICI therapeutics for each of the cancers and interestingly there were relatively more approvals for the athero-dissimilar cancers, suggesting that stimulating these immune pathways may indeed be more beneficial in the athero-dissimilar cancers (Figure S4). We also observed several other differences between athero-similar and dissimilar cancers including DNA repair, cell cycle regulatory pathways, and transcription factors MYC and E2F (Figure 2C). Notably, the athero-dissimilar cancers had significantly worse survival compared to athero-similar cancers (Figure 2D).

Using the drug prediction software, OCTAD, to analyze transcriptional risk profiles reveals numerous well characterized drugs, which may be able to simultaneously treat cancer and atherosclerotic CVD

Having characterized the pathogenic similarities between atherosclerosis and cancer, we sought to leverage this information by using the drug repurposing algorithm, OCTAD, to identify potential drugs that could theoretically provide benefit to both cancer and atherosclerosis (Figure 3A).[24] In brief, reverse gene expression scores (RGES) were calculated based on how effectively disease gene expression signatures could be "reversed" by transcriptional changes induced by the thousands of compounds found in the Library of Integrated Network-Based Cellular Signatures (LINCS).[25] Compounds with negative RGES values are predicted to reverse the disease signature and thus may be useful putative therapies.

OCTAD was originally built to use a disease gene expression signature derived from the comparison of diseased tissue with neighboring healthy tissue. To repurpose this strategy in a more clinically useful manner, we generated disease gene expression scores comparing tumors with good or bad prognoses. In a similar manner, we generated atherosclerosis disease gene expression scores by comparing the two extremes of the atherosclerotic CVD risk axes (e.g., non-atherosclerotic mammary artery versus diseased

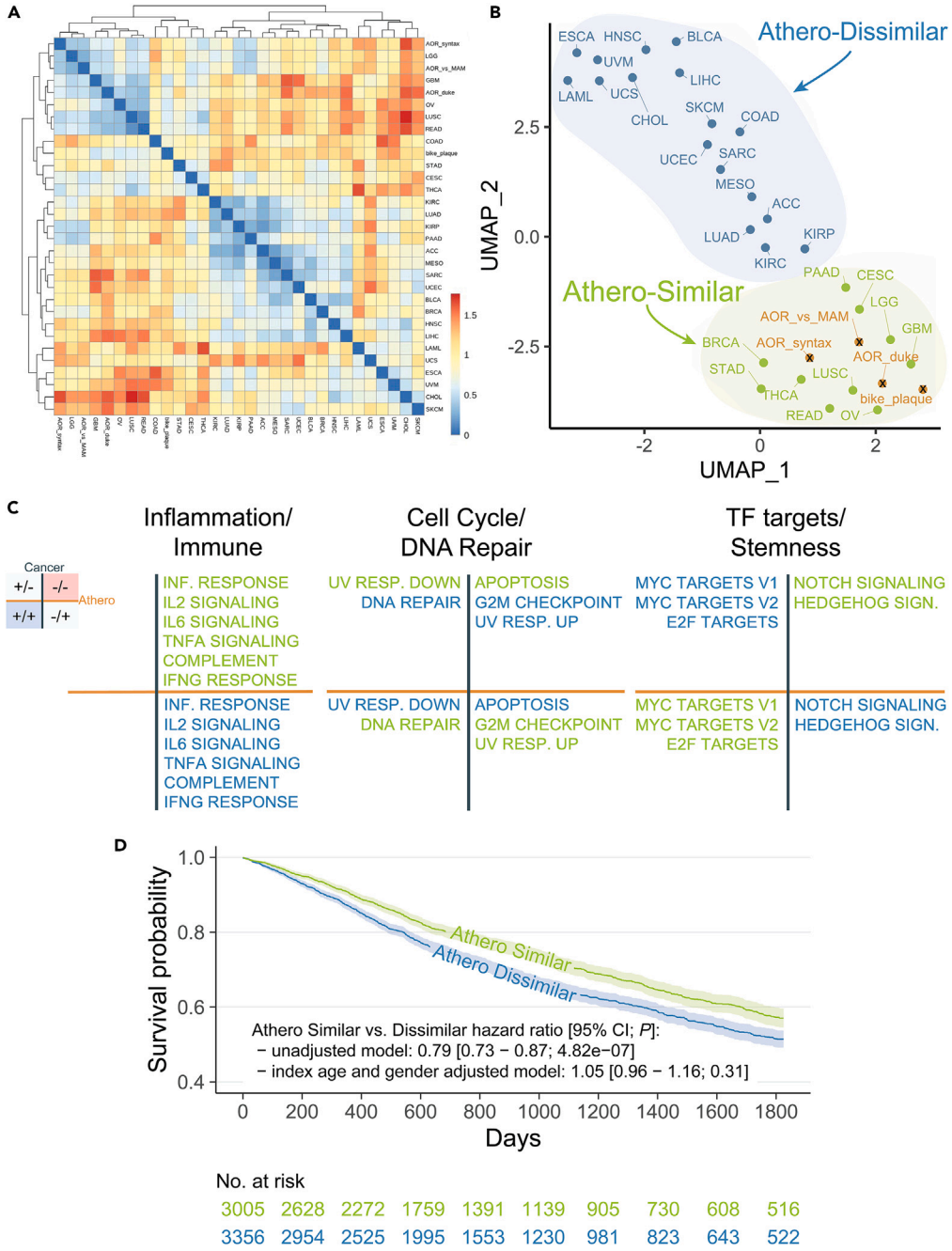

Figure 2. Clustering of cancers based on Hallmark pathway enrichment suggests that certain cancers are more transcriptionally similar to atherosclerosis

(A) Heatmap of Hallmark pathway enrichment (cancer abbreviations can be found in Figure S1).

(B) UMAP of atherosclerosis and cancer datasets with clustering revealing that certain cancers cluster closely with the atherosclerosis datasets (highlighted in orange), which were termed athero-similar (highlighted in green) and athero-dissimilar (highlighted in blue).

(C) Highlights of important differences between the two groups of cancers including in inflammatory pathways, response to DNA damage, cell cycle regulation, and gene targets of MYC and E2F and cell differentiation signaling. For full pathway quadrant plots, refer to Figure S3.

(D) Kaplan-Meier graph of aggregate patient survival in the athero-similar and -dissimilar cancer groups showing a significantly worse survival in patients with athero-dissimilar cancers in the unadjusted model.

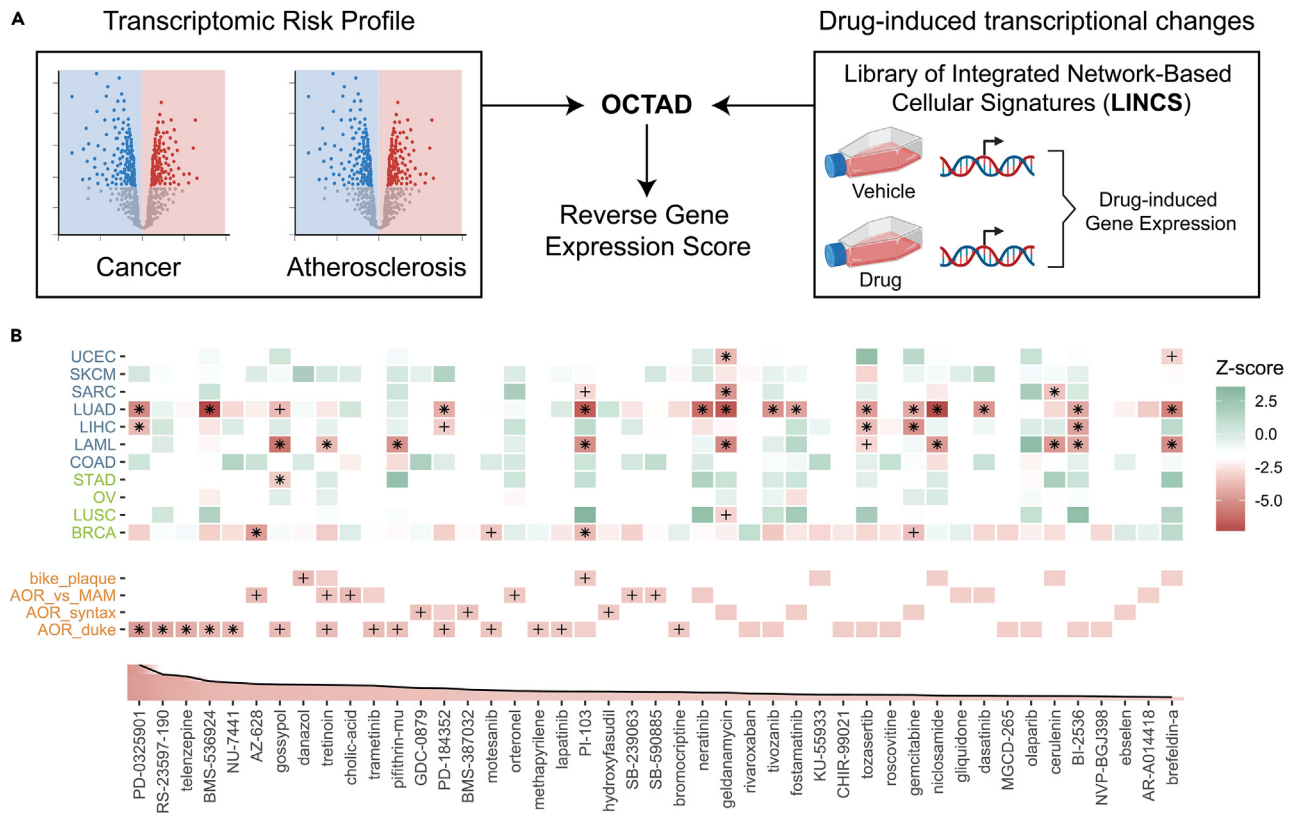

Figure 3. Leveraging transcriptomic risk profiles to identify compounds that may yield benefit in atherosclerosis and cancer

(A) Schematic demonstrating the integration of transcriptomic risk profiles and the Library of Integrated Network-based Cellular Signatures (LINCS) using the OCTAD algorithm to identify compounds predicted to reverse pathogenic transcriptional signatures.

(B) A heatmap of the top 45 compounds predicted to benefit the atherosclerosis datasets. Those with negative Z scores (red) are predicted to be beneficial. Notably, there are numerous compounds predicted to benefit atherosclerosis and individual cancers. These drugs may represent novel compounds that could provide mutual benefit across both diseases. *: adjusted p value <0.1. +: adjusted p value <0.5.

aortic sinus or low-versus high- DUKE scores). Of the 1,719 compounds, 510 had an RGES with an unadjusted p value of <0.05 in one of the CAD datasets however none of them were significant by multiple comparisons (Holm's correction), which was thought to be due to limitations in matching LINCS cell lines with *in vivo* atherosclerotic lesions. Therefore, the OCTAD predictions are exploratory and hypothesis generating. Despite these limitations, OCTAD correctly predicted numerous well-known cardioprotective medications. For example, among the compounds with $p < 0.05$ in one of the atherosclerosis datasets were many well-documented cardioprotective medications including several statins (atorvastatin, lovastatin, and simvastatin), carvedilol, losartan, and hydrochlorothiazide.

The top performing medications predicted to improve atherosclerosis are largely still in clinical trials. The top performer, PD0325901, was 1 of 3 MEK inhibitors found in the top 45 medications (Figure 3B). Interestingly treatment with a MEK inhibitor has previously been shown to reduce atherosclerosis development in ApoE$^{-/-}$ mice when also administered with an LXR agonist, which was thought to be mediated by enhanced inflammation resolution by macrophages.[26,27] Given that this strategy only interrogates the transcriptome of the atherosclerotic lesion itself and therefore would miss any extra-lesional processes that contribute to cardiovascular events (e.g., coagulation cascade), it is not surprising that some medications with known pro-atherogenic influence (e.g., celecoxib and cholic acid) were also found on the list. Despite this limitation, however, there were many compounds that match preclinical observations. For example, several vitamin A analogs were found in the list, which have been shown to exert anti-atherosclerotic properties in murine atherosclerosis.[28,29] Other examples of preclinical benefit include the p38 inhibitor (SB-239063),[30] the HSP90 inhibitor (geldanamycin),[31] the factor Xa inhibitor (rivaroxaban),[32] the SYK inhibitor (fostamatinib),[33] the tyrosine kinase inhibitor (dasatinib),[34] and the GPx1 mimetic (ebselen).[35]

In addition, there were numerous medications predicted to be beneficial for atherosclerosis and certain cancers. For example, the MEK inhibitor (PD0325901) was predicted to be beneficial in atherosclerosis as well as lung adenocarcinoma (LUAD) and hepatocellular carcinoma (LIHC). This same compound was recently shown to improve the efficacy of PD-1 inhibitors in non-small cell lung cancer[36] and has been shown to reduce HCC tumor growth in murine models.[37] Tretinoin (also known as all-trans retinoic acid) was predicted to be beneficial in 3 out of the 4 atherosclerosis datasets and the algorithm predicts it to be beneficial in acute myeloid leukemia (LAML). Notably, all-trans retinoic acid is the first line treatment for a subtype of LAML, acute promyelocytic leukemia. Taken together, these data suggest that using transcriptomic data correlated with disease severity can be a useful strategy to identify therapeutic targets for both atherosclerosis and cancer (see full list of compounds and predictions in Table S1).

DISCUSSION

Cancer and atherosclerosis have many overlapping features. While it has been recognized that both diseases share risk factors and pathogenic drivers, a comprehensive analysis of shared dysregulated processes that drive both diseases has never been performed. In this hypothesis-generating manuscript, we sought to exploit the substantial progress that has been made in understanding the transcriptomics of both diseases, and then to use this knowledge to define and prioritize shared pathways for translational targeting. In doing so, we have made several important observations: **First**, when the transcriptional profiles of all cancers are compared with atherosclerosis, multiple commonly dysregulated pathways were identified which appeared to exacerbate both conditions including glycolytic metabolism, hypoxia, and EMT. **Second**, we show that certain cancers are indistinguishable from atherosclerosis based on their transcriptional risk profiles, meaning that the same transcriptional pathways correlate with disease severity/survival in these particular malignancies. **Third**, we identify key differences between athero-similar and -dissimilar cancers with important implications including that athero-promoting inflammatory pathways are also detrimental in athero-similar but protective in athero-dissimilar cancers. **Fourth**, we leverage the drug repurposing algorithm, OCTAD, to identify compounds that are predicted to reverse the disease gene expression score for both atherosclerosis and cancer, highlighting potential opportunities for the repurposing of drugs across each disease state.

Scientists and clinicians have contemplated the similarities between cancer and atherosclerosis for decades.[38] For example, both diseases have common heritable genetic factors which predispose to disease development. Interestingly, the top GWAS hit for CAD at 9p21 is found at a locus which encodes for the key tumor suppressor gene, CDKN2B. Both diseases share lengthy incubation periods and can recur many years after their initial clinical manifestation. The similarities are particularly striking at a cellular level. Indeed, the lexicon used to describe the microenvironments of a tumor and an atheroma include similar phrases like plasticity, inflammation, cell cycle dysregulation, and metabolic disarray.[39,40] Both have a pathogenic macrophage population (tumor associated macrophages versus foam cells), a critical reliance on extracellular matrix deposition (tumor microenvironment versus fibrous cap), necrotic foci (tumor necrosis versus necrotic core), a clonal origin (tumor cells versus SMC clonal expansion), and both are chronic nonresolving cellular stress characterized by a diverse set of cell populations.

We have previously investigated the genetic overlap of cancer and CAD by testing the hypothesis that their similarities are mediated, in part, through shared genetic predisposition.[41] To our surprise, we found that the majority of cancers had no genetic correlation with CAD. This suggests that the similarities observed in the current report are more likely mediated by shared dysregulated processes which occur at the transcriptional level and beyond. The question remains whether the shared pathogenic processes could allow for the existence of one of these pathogenic states to exacerbate the development or complications of the other. Interestingly, there is now emerging evidence to suggest that those patients with CVD are at higher risk for cancer development even after controlling for their shared risk factors.[42] It has been posited that secreted factors including extracellular vesicles, circulating immune populations, or substrate availability could mediate this pathogenic communication. These unanswered questions remain the focus of intense pre-clinical evaluation.

In conclusion, this study intersects transcriptomic datasets from human cancer and cardiovascular patients to uncover shared pathogenic features of both diseases. Future studies may be able to leverage these commonalities to prioritize translational targets to usher in a new frontier for cardio-oncology, where mutual benefit across both disease states is the goal.

Limitations of the study

There are several notable limitations of our study. First, this study was made possible by the pioneering efforts of the STARNET and BiKE datasets and, despite being industry-leading, they are dwarfed in statistical power by those in the cancer field. Second, unlike the endpoint of mortality that has been used in TCGA, we are forced to use less rigid endpoints like disease-severity scores, healthy-versus-diseased tissue, and prospective MACE rates when studying cardiovascular outcomes. Third, due to our focus on transcriptomic changes of the atherosclerotic lesion, we have a myopic view of the processes involved in CVD and are unable to account for other important factors like cardiomyocyte health, electrophysiologic impacts, and the coagulation cascade, all of which are known to be critically important in assessing the cardiotoxic effects of cancer therapeutics.

STAR★METHODS

Detailed methods are provided in the online version of this paper and include the following:

- KEY RESOURCES TABLE
- RESOURCE AVAILABILITY
  - Lead contact
  - Materials availability
  - Data and code availability
- EXPERIMENTAL MODEL AND STUDY PARTICIPANT DETAILS
  - Study populations
- METHOD DETAILS
  - Survival and gene-set enrichment analyses
  - Identifying shared pathways between atherosclerosis and cancer
  - Clustering individual disease datasets
  - Estimating immune cell investment
  - Tabulating ICI FDA approval history by cancer
  - In-silico drug screening to identify putative therapeutic compounds
- QUANTIFICATION AND STATISTICAL ANALYSIS

SUPPLEMENTAL INFORMATION

Supplemental information can be found online at https://doi.org/10.1016/j.isci.2023.107513.

ACKNOWLEDGMENTS

Funding.

Dr. Baylis was supported by NIH F30HL136188. Dr. Leeper is supported by NIH R35HL144475 and AHA EIA34770065. Drs. Leeper and Björkegren are supported by Leducq Foundation PlaqOmics consortia (18CVD02).

AUTHOR CONTRIBUTIONS

R.A.B., H.G., and N.L. conceptualized the project, designed the experimental approach, and wrote the manuscript. H.G. performed the bioinformatics. H.G. and R.A.B. generated the figures. F.W., C.B., L.L. provided critical insights and assisted to manuscript preparation. J.B. provided critical insights into atherosclerotic transcriptomics, experimental design, and integration of STARNET data. N.L. supervised the project and had a critical role in experimental design, data interpretation, manuscript writing, and funding the project.

DECLARATION OF INTERESTS

The authors have declared that no conflict of interest exists.

Received: March 20, 2023
Revised: June 18, 2023
Accepted: July 27, 2023
Published: July 29, 2023

REFERENCES

1. Handy, C.E., Quispe, R., Pinto, X., Blaha, M.J., Blumenthal, R.S., Michos, E.D., Lima, J.A.C., Guallar, E., Ryu, S., Cho, J., et al. (2018). Synergistic Opportunities in the Interplay Between Cancer Screening and Cardiovascular Disease Risk Assessment: Together We Are Stronger. Circulation *138*, 727–734. https://doi.org/10.1161/CIRCULATIONAHA.118.035516.

2. Dutta, P., Courties, G., Wei, Y., Leuschner, F., Gorbatov, R., Robbins, C.S., Iwamoto, Y., Thompson, B., Carlson, A.L., Heidt, T., et al. (2012). Myocardial infarction accelerates atherosclerosis. Nature *487*, 325–329. https://doi.org/10.1038/nature11260.

3. Koelwyn, G.J., Newman, A.A.C., Afonso, M.S., van Solingen, C., Corr, E.M., Brown, E.J., Albers, K.B., Yamaguchi, N., Narke, D., Schlegel, M., et al. (2020). Myocardial infarction accelerates breast cancer via innate immune reprogramming. Nat. Med. *26*, 1452–1458. https://doi.org/10.1038/s41591-020-0964-7.

4. Ringel, A.E., Drijvers, J.M., Baker, G.J., Catozzi, A., García-Cañaveras, J.C., Gassaway, B.M., Miller, B.C., Juneja, V.R., Nguyen, T.H., Joshi, S., et al. (2020). Obesity Shapes Metabolism in the Tumor Microenvironment to Suppress Anti-Tumor Immunity. Cell *183*, 1848–1866.e26. https://doi.org/10.1016/j.cell.2020.11.009.

5. Ridker, P.M., MacFadyen, J.G., Thuren, T., Everett, B.M., Libby, P., Glynn, R.J., CANTOS Trial Group, Lorenzatti, A., Krum, H., Varigos, J., et al. (2017). Effect of interleukin-1β inhibition with canakinumab on incident lung cancer in patients with atherosclerosis: exploratory results from a randomised, double-blind, placebo-controlled trial. Lancet *390*, 1833–1842. https://doi.org/10.1016/S0140-6736(17)32247-X.

6. Ridker, P.M., Everett, B.M., Thuren, T., MacFadyen, J.G., Chang, W.H., Ballantyne, C., Fonseca, F., Nicolau, J., Koenig, W., Anker, S.D., et al. (2017). Antiinflammatory Therapy with Canakinumab for Atherosclerotic Disease. N. Engl. J. Med. *377*, 1119–1131. https://doi.org/10.1056/NEJMoa1707914.

7. Paz-Ares, L., Goto, Y., Lim, W.D.T., Halmos, B., Cho, B.C., Dols, M.C., Gonzalez-Larriba, J.L., Zhou, C., Demedts, I., Atmaca, A., et al. (2021). 1194MO Canakinumab (CAN) + docetaxel (DTX) for the second- or third-line (2/3L) treatment of advanced non-small cell lung cancer (NSCLC): CANOPY-2 phase III results. Ann. Oncol. *32*, S953–S954. https://doi.org/10.1016/j.annonc.2021.08.1799.

8. Jarr, K.-U., Nakamoto, R., Doan, B.H., Kojima, Y., Weissman, I.L., Advani, R.H., Iagaru, A., and Leeper, N.J. (2021). Effect of CD47 Blockade on Vascular Inflammation. N. Engl. J. Med. *384*, 382–383. https://doi.org/10.1056/NEJMc2029834.

9. Robert, C. (2020). A decade of immune-checkpoint inhibitors in cancer therapy. Nat. Commun. *11*, 3801. https://doi.org/10.1038/s41467-020-17670-y.

10. Hu, J.-R., Florido, R., Lipson, E.J., Naidoo, J., Ardehali, R., Tocchetti, C.G., Lyon, A.R., Padera, R.F., Johnson, D.B., and Moslehi, J. (2019). Cardiovascular toxicities associated with immune checkpoint inhibitors. Cardiovasc. Res. *115*, 854–868. https://doi.org/10.1093/cvr/cvz026.

11. Drobni, Z.D., Alvi, R.M., Taron, J., Zafar, A., Murphy, S.P., Rambarat, P.K., Mosarla, R.C., Lee, C., Zlotoff, D.A., Raghu, V.K., et al. (2020). Association Between Immune Checkpoint Inhibitors With Cardiovascular Events and Atherosclerotic Plaque. Circulation *142*, 2299–2311. https://doi.org/10.1161/CIRCULATIONAHA.120.049981.

12. Poels, K., Neppelenbroek, S.I.M., Kersten, M.J., Antoni, M.L., Lutgens, E., and Seijkens, T.T.P. (2021). Immune checkpoint inhibitor treatment and atherosclerotic cardiovascular disease: an emerging clinical problem. J. Immunother. Cancer *9*, e002916. https://doi.org/10.1136/jitc-2021-002916.

13. Franzén, O., Ermel, R., Cohain, A., Akers, N.K., Di Narzo, A., Talukdar, H.A., Foroughi-Asl, H., Giambartolomei, C., Fullard, J.F., Sukhavasi, K., et al. (2016). Cardiometabolic risk loci share downstream cis- and trans-gene regulation across tissues and diseases. Science *353*, 827–830. https://doi.org/10.1126/science.aad6970.

14. Mark, D.B., Nelson, C.L., Califf, R.M., Harrell, F.E., Lee, K.L., Jones, R.H., Fortin, D.F., Stack, R.S., Glower, D.D., and Smith, L.R. (1994). Continuing evolution of therapy for coronary artery disease. Initial results from the era of coronary angioplasty. Circulation *89*, 2015–2025. https://doi.org/10.1161/01.CIR.89.5.2015.

15. Sianos, G., Morel, M.-A., Kappetein, A.P., Morice, M.-C., Colombo, A., Dawkins, K., van den Brand, M., Van Dyck, N., Russell, M.E., Mohr, F.W., and Serruys, P.W. (2005). The SYNTAX Score: an angiographic tool grading the complexity of coronary artery disease. EuroIntervention. *1*, 219–227.

16. Folkersen, L., Persson, J., Ekstrand, J., Agardh, H.E., Hansson, G.K., Gabrielsen, A., Hedin, U., and Paulsson-Berne, G. (2012). Prediction of Ischemic Events on the Basis of Transcriptomic and Genomic Profiling in Patients Undergoing Carotid Endarterectomy. Mol. Med. *18*, 669–675. https://doi.org/10.2119/molmed.2011.00479.

17. Tomas, L., Edsfeldt, A., Mollet, I.G., Perisic Matic, L., Prehn, C., Adamski, J., Paulsson-Berne, G., Hedin, U., Nilsson, J., Bengtsson, E., et al. (2018). Altered metabolism distinguishes high-risk from stable carotid atherosclerotic plaques. Eur. Heart J. *39*, 2301–2310. https://doi.org/10.1093/eurheartj/ehy124.

18. Chen, P.-Y., Qin, L., Baeyens, N., Li, G., Afolabi, T., Budatha, M., Tellides, G., Schwartz, M.A., and Simons, M. (2015). Endothelial-to-mesenchymal transition drives atherosclerosis progression. J. Clin. Invest. *125*, 4514–4528. https://doi.org/10.1172/JCI82719.

19. Evrard, S.M., Lecce, L., Michelis, K.C., Nomura-Kitabayashi, A., Pandey, G., Purushothaman, K.-R., d'Escamard, V., Li, J.R., Hadri, L., Fujitani, K., et al. (2016). Endothelial to mesenchymal transition is common in atherosclerotic lesions and is associated with plaque instability. Nat. Commun. *7*, 11853. https://doi.org/10.1038/ncomms11853.

20. Low, E.L., Baker, A.H., and Bradshaw, A.C. (2019). TGFβ, smooth muscle cells and coronary artery disease: a review. Cell. Signal. *53*, 90–101. https://doi.org/10.1016/j.cellsig.2018.09.004.

21. McInnes, L., Healy, J., and Melville, J. (2018). UMAP: Uniform Manifold Approximation and Projection for Dimension Reduction. https://doi.org/10.48550/ARXIV.1802.03426.

22. Wang, Y., Nanda, V., Direnzo, D., Ye, J., Xiao, S., Kojima, Y., Howe, K.L., Jarr, K.-U., Flores, A.M., Tsantilas, P., et al. (2020). Clonally expanding smooth muscle cells promote atherosclerosis by escaping efferocytosis and activating the complement cascade. Proc. Natl. Acad. Sci. *117*, 15818–15826. https://doi.org/10.1073/pnas.2006348117.

23. Roumenina, L.T., Daugan, M.V., Petitprez, F., Sautès-Fridman, C., and Fridman, W.H. (2019). Context-dependent roles of complement in cancer. Nat. Rev. Cancer *19*, 698–715. https://doi.org/10.1038/s41568-019-0210-0.

24. Zeng, B., Glicksberg, B.S., Newbury, P., Chekalin, E., Xing, J., Liu, K., Wen, A., Chow, C., and Chen, B. (2021). OCTAD: an open workspace for virtually screening therapeutics targeting precise cancer patient groups using gene expression features. Nat. Protoc. *16*, 728–753. https://doi.org/10.1038/s41596-020-00430-z.

25. Keenan, A.B., Jenkins, S.L., Jagodnik, K.M., Koplev, S., He, E., Torre, D., Wang, Z., Dohlman, A.B., Silverstein, M.C., Lachmann, A., et al. (2018). The Library of Integrated Network-Based Cellular Signatures NIH Program: System-Level Cataloging of Human Cells Response to Perturbations. Cell Syst. *6*, 13–24. https://doi.org/10.1016/j.cels.2017.11.001.

26. Chen, Y., Duan, Y., Yang, X., Sun, L., Liu, M., Wang, Q., Ma, X., Zhang, W., Li, X., Hu, W., et al. (2015). Inhibition of ERK1/2 and activation of LXR synergistically reduce atherosclerotic lesions in ApoE-deficient mice. Arterioscler. Thromb. Vasc. Biol. *35*, 948–959. https://doi.org/10.1161/ATVBAHA.114.305116.

27. Long, M.E., Eddy, W.E., Gong, K.-Q., Lovelace-Macon, L.L., McMahan, R.S., Charron, J., Liles, W.C., and Manicone, A.M. (2017). MEK1/2 Inhibition Promotes Macrophage Reparative Properties. J. Immunol. Baltim. Md. *198*, 862–872. https://doi.org/10.4049/jimmunol.1601059.

28. Kalisz, M., Chmielowska, M., Martyńska, L., Domańska, A., Bik, W., and Litwiniuk, A. (2021). All-trans-retinoic acid ameliorates atherosclerosis, promotes perivascular

adipose tissue browning, and increases adiponectin production in Apo-E mice. Sci. Rep. *11*, 4451. https://doi.org/10.1038/s41598-021-83939-x.

29. Pan, H., Xue, C., Auerbach, B.J., Fan, J., Bashore, A.C., Cui, J., Yang, D.Y., Trignano, S.B., Liu, W., Shi, J., et al. (2020). Single-Cell Genomics Reveals a Novel Cell State During Smooth Muscle Cell Phenotypic Switching and Potential Therapeutic Targets for Atherosclerosis in Mouse and Human. Circulation *142*, 2060–2075. https://doi.org/10.1161/CIRCULATIONAHA.120.048378.

30. Morris, J.B., Olzinski, A.R., Bernard, R.E., Aravindhan, K., Mirabile, R.C., Boyce, R., Willette, R.N., and Jucker, B.M. (2008). p38 MAPK Inhibition Reduces Aortic Ultrasmall Superparamagnetic Iron Oxide Uptake in a Mouse Model of Atherosclerosis: MRI Assessment. Arterioscler. Thromb. Vasc. Biol. *28*, 265–271. https://doi.org/10.1161/ATVBAHA.107.151175.

31. Madrigal-Matute, J., López-Franco, O., Blanco-Colio, L.M., Muñoz-García, B., Ramos-Mozo, P., Ortega, L., Egido, J., and Martín-Ventura, J.L. (2010). Heat shock protein 90 inhibitors attenuate inflammatory responses in atherosclerosis. Cardiovasc. Res. *86*, 330–337. https://doi.org/10.1093/cvr/cvq046.

32. Ito, Y., Maejima, Y., Nakagama, S., Shiheido-Watanabe, Y., Tamura, N., and Sasano, T. (2021). Rivaroxaban, a Direct Oral Factor Xa Inhibitor, Attenuates Atherosclerosis by Alleviating Factor Xa–PAR2-Mediated Autophagy Suppression. JACC. Basic Transl. Sci. *6*, 964–980. https://doi.org/10.1016/j.jacbts.2021.09.010.

33. Hilgendorf, I., Eisele, S., Remer, I., Schmitz, J., Zeschky, K., Colberg, C., Stachon, P., Wolf, D., Willecke, F., Buchner, M., et al. (2011). The Oral Spleen Tyrosine Kinase Inhibitor Fostamatinib Attenuates Inflammation and Atherogenesis in Low-Density Lipoprotein Receptor–Deficient Mice. Arterioscler. Thromb. Vasc. Biol. *31*, 1991–1999. https://doi.org/10.1161/ATVBAHA.111.230847.

34. Takaba, M., Iwaki, T., Arakawa, T., Ono, T., Maekawa, Y., and Umemura, K. (2022). Dasatinib suppresses atherosclerotic lesions by suppressing cholesterol uptake in a mouse model of hypercholesterolemia. J. Pharmacol. Sci. *149*, 158–165. https://doi.org/10.1016/j.jphs.2022.04.009.

35. Chew, P., Yuen, D.Y.C., Stefanovic, N., Pete, J., Coughlan, M.T., Jandeleit-Dahm, K.A., Thomas, M.C., Rosenfeldt, F., Cooper, M.E., and de Haan, J.B. (2010). Antiatherosclerotic and Renoprotective Effects of Ebselen in the Diabetic Apolipoprotein E/GPx1-Double Knockout Mouse. Diabetes *59*, 3198–3207. https://doi.org/10.2337/db10-0195.

36. Luo, M., Xia, Y., Wang, F., Zhang, H., Su, D., Su, C., Yang, C., Wu, S., An, S., Lin, S., and Fu, L. (2021). PD0325901, an ERK inhibitor, enhances the efficacy of PD-1 inhibitor in non-small cell lung carcinoma. Acta Pharm. Sin. B *11*, 3120–3133. https://doi.org/10.1016/j.apsb.2021.03.010.

37. Hennig, M., Yip-Schneider, M.T., Wentz, S., Wu, H., Hekmatyar, S.K., Klein, P., Bansal, N., and Schmidt, C.M. (2010). Targeting mitogen-activated protein kinase kinase with the inhibitor PD0325901 decreases hepatocellular carcinoma growth in vitro and in mouse model systems. Hepatology *51*, 1218–1225. https://doi.org/10.1002/hep.23470.

38. Ross, J.S., Stagliano, N.E., Donovan, M.J., Breitbart, R.E., and Ginsburg, G.S. (2001). Atherosclerosis and cancer: common molecular pathways of disease development and progression. Ann. N. Y. Acad. Sci. *947*, 271–292. discussion 292-293.

39. DiRenzo, D., Owens, G.K., and Leeper, N.J. (2017). "Attack of the Clones": Commonalities Between Cancer and Atherosclerosis. Circ. Res. *120*, 624–626. https://doi.org/10.1161/CIRCRESAHA.116.310091.

40. Libby, P., and Kobold, S. (2019). Inflammation: a common contributor to cancer, aging, and cardiovascular diseases—expanding the concept of cardio-oncology. Cardiovasc. Res. *115*, 824–829. https://doi.org/10.1093/cvr/cvz058.

41. Baylis, R.A., Wang, F., Gao, H., Bell, C., Luo, L., Nead, K.T., Neilan, T.G., Ross, E.G., Klarin, D., and Leeper, N.J. (2022). Coronary artery disease and prostate cancer share a common genetic risk mediated through Lipoprotein(a). Cardiovascular Medicine. https://doi.org/10.1101/2022.11.08.22282072.

42. Bell, C.F., Lei, X., Haas, A., Baylis, R.A., Gao, H., Luo, L., Giordano, S.H., Wehner, M.R., Nead, K.T., and Leeper, N.J. (2023). Risk of Cancer After Diagnosis of Cardiovascular Disease. JACC CardioOncology. S2666087323000583. https://doi.org/10.1016/j.jaccao.2023.01.010.

43. Colaprico, A., Silva, T.C., Olsen, C., Garofano, L., Cava, C., Garolini, D., Sabedot, T.S., Malta, T.M., Pagnotta, S.M., Castiglioni, I., et al. (2016). TCGAbiolinks: an R/Bioconductor package for integrative analysis of TCGA data. Nucleic Acids Res. *44*, e71. https://doi.org/10.1093/nar/gkv1507.

44. Therneau, T.M. (2021). A Package for Survival Analysis in R.

45. Wu, T., Hu, E., Xu, S., Chen, M., Guo, P., Dai, Z., Feng, T., Zhou, L., Tang, W., Zhan, L., et al. (2021). clusterProfiler 4.0: A universal enrichment tool for interpreting omics data. Innovation *2*, 100141. https://doi.org/10.1016/j.xinn.2021.100141.

46. Hao, Y., Hao, S., Andersen-Nissen, E., Mauck, W.M., Zheng, S., Butler, A., Lee, M.J., Wilk, A.J., Darby, C., Zager, M., et al. (2021). Integrated analysis of multimodal single-cell data. Cell *184*, 3573–3587.e29. https://doi.org/10.1016/j.cell.2021.04.048.

47. Goldman, M.J., Craft, B., Hastie, M., Repečka, K., McDade, F., Kamath, A., Banerjee, A., Luo, Y., Rogers, D., Brooks, A.N., et al. (2020). Visualizing and interpreting cancer genomics data via the Xena platform. Nat. Biotechnol. *38*, 675–678. https://doi.org/10.1038/s41587-020-0546-8.

48. Subramanian, A., Narayan, R., Corsello, S.M., Peck, D.D., Natoli, T.E., Lu, X., Gould, J., Davis, J.F., Tubelli, A.A., Asiedu, J.K., et al. (2017). A Next Generation Connectivity Map: L1000 Platform and the First 1,000,000 Profiles. Cell *171*, 1437–1452.e17. https://doi.org/10.1016/j.cell.2017.10.049.

49. Cancer Genome Atlas Research Network, Weinstein, J.N., Collisson, E.A., Mills, G.B., Shaw, K.R.M., Ozenberger, B.A., Ellrott, K., Shmulevich, I., Sander, C., and Stuart, J.M. (2013). The Cancer Genome Atlas Pan-Cancer analysis project. Nat. Genet. *45*, 1113–1120. https://doi.org/10.1038/ng.2764.

50. Koplev, S., Seldin, M., Sukhavasi, K., Ermel, R., Pang, S., Zeng, L., Bankier, S., Di Narzo, A., Cheng, H., Meda, V., et al. (2022). A mechanistic framework for cardiometabolic and coronary artery diseases. Nat. Cardiovasc. Res. *1*, 85–100. https://doi.org/10.1038/s44161-021-00009-1.

51. Liberzon, A., Birger, C., Thorvaldsdóttir, H., Ghandi, M., Mesirov, J.P., and Tamayo, P. (2015). The Molecular Signatures Database (MSigDB) hallmark gene set collection. Cell Syst. *1*, 417–425. https://doi.org/10.1016/j.cels.2015.12.004.

52. Miao, Y.R., Zhang, Q., Lei, Q., Luo, M., Xie, G.Y., Wang, H., and Guo, A.Y. (2020). ImmuCellAI: A Unique Method for Comprehensive T-Cell Subsets Abundance Prediction and its Application in Cancer Immunotherapy. Adv. Sci. *7*, 1902880. https://doi.org/10.1002/advs.201902880.

53. Liu, C.-J., Hu, F.-F., Xie, G.-Y., Miao, Y.-R., Li, X.-W., Zeng, Y., and Guo, A.-Y. (2023). GSCA: an integrated platform for gene set cancer analysis at genomic, pharmacogenomic and immunogenomic levels. Brief. Bioinform. *24*, bbac558. https://doi.org/10.1093/bib/bbac558.

STAR★METHODS

KEY RESOURCES TABLE

REAGENT or RESOURCE	SOURCE	IDENTIFIER
Software and algorithms		
R TCGAbiolinks package	Colaprico et al.[43]	https://doi.org/10.18129/B9.bioc.TCGAbiolinks
R survival package	Therneau et al.[44]	https://github.com/therneau/survival
R clusterProfiler package	Wu et al.[45]	https://doi.org/10.18129/B9.bioc.clusterProfiler
R Seurat package	Hao et al.[46]	https://github.com/satijalab/seurat
OCTAD algorithm	Zeng[24]	https://github.com/Bin-Chen-Lab/octad
Other		
TCGA Pan-Cancer gene expression profiles	UCSC Xena[47]	https://xenabrowser.net/datapages/?cohort=GDC%20Pan-Cancer%20(PANCAN)
BiKE dataset	NCBI GEO (GSE21545)	https://www.ncbi.nlm.nih.gov/geo/query/acc.cgi?acc=GSE21545
The association summary statistics for the gene expression against the DUKE CAD Severity Score or angiographic CAD SYNTAX Score	STARNET[13]	
The differential expression summary statistics for the mammary artery (non-atherosclerotic) vs. aortic sinus (atherosclerotic)	STARNET[13]	
LINCS L1000 mRNA profiling dataset	Subramanian[48]	https://lincsportal.ccs.miami.edu/dcic-portal

RESOURCE AVAILABILITY

Lead contact

Further information and requests for resources should be directed to and will be fulfilled by the lead contact, Dr. Nicholas J. Leeper (nleeper@stanford.edu).

Materials availability

The study did not generate new materials.

Data and code availability

- This paper does not report the original code.
- The sources of the datasets supporting the current study are presented in the "key resources table" and "STAR Methods" sections.
- Any additional information required to reanalyze the data reported in this paper or reproduce the results is available from the lead contact upon request.

EXPERIMENTAL MODEL AND STUDY PARTICIPANT DETAILS

Study populations

The Cancer Genome Atlas (TCGA) has accumulated genomic and transcriptomic data from over 11,000 tumors and 33 cancer types.[49] Importantly, the database also includes patient survival data such that tumor gene expression can be correlated with survival. The Stockholm-Tartu Atherosclerosis Reverse Networks Engineering Task (STARNET) dataset includes RNA sequencing data on 600 patients from tissue collected at the time of coronary artery bypass. Relevant data to this study includes atherosclerotic aortic root (AOR) and disease-free internal mammary artery (MAM).[50] The Biobank of Karolinska Endarterectomies (BiKE) includes transcriptomic data from 126 carotid plaques removed during carotid endarterectomy.[16] These

datasets have previously been published and include more detailed demographic breakdown, which can be found in the references in the key resources table. All patient data used in this manuscript was provided in a de-identified format without access to identification key and therefore was exempt from IRB review.

METHOD DETAILS

Survival and gene-set enrichment analyses

To correlate transcriptional data with survival, multivariate Cox regression was performed using the R survival package on the TCGA and BiKE datasets with gender and age at index as covariates.[44] To improve interpretation and move from individual gene level to pathway level, hallmark gene set enrichment analysis (GSEA)[51] was performed on the summary statistics (Cox regression coefficient) using the R clusterProfiler package.[45] The STARNET datasets were shared as summary statistics and therefore GSEA was directly applied using the correlation coefficient or the log2 fold change as input. The GSEA analysis provides a normalized enrichment score (NES), which compares the sample to the mean enrichment of a random sample the same size and allows GSEA to determine significance. For this study, a positive NES indicates that this particular pathway has more genes that correlated with worsening disease severity meaning it had a positive Cox coefficient, positive correlation with the severity score (i.e., DUKE or SYNTAX), or positive log2 fold change.

Identifying shared pathways between atherosclerosis and cancer

To understand the overall impact of a transcriptional pathway to atherosclerosis or cancer, the mean NES was calculated for each disease. If the average NES for the disease was positive, that pathway was considered to be overall detrimental to the disease (positive on the X-axis for atherosclerosis or the Y-axis for cancer) whereas a negative average NES was beneficial (negative on the X-axis for atherosclerosis or Y-axis for cancer). The same logic was applied to the athero-similar and -dissimilar plots in Figure S3.

Clustering individual disease datasets

To understand the relationship of the correlation of transcriptomic pathways and disease severity between the datasets, each individual dataset was plotted on a UMAP based on their NES matrix. The shared nearest neighbor clustering algorithm from the R Seurat package[46] was then applied to identify potential clusters using the following parameters (npcs 20, n.neighbors 5, k.param 5, and resolution 0.4), which resolved two clusters (one which included all of the atherosclerosis datasets [termed athero-similar] and another that did not include any atherosclerosis datasets [termed athero-dissimilar]).

Estimating immune cell investment

To determine if differences in the abundance of immune cell populations could be driving the transcriptional differences observed between athero-similar and -dissimilar cancers, the ImmuCellAI[52] estimates for immune cell infiltration in the TCGA tumor samples were obtained from the Gene Set Cancer Analysis (GSCA) website,[53] aggregated to the mean values across each cancer type, and then compared between the two clusters of cancers by t-test.

Tabulating ICI FDA approval history by cancer

To determine the frequency of immune checkpoint inhibitor FDA approvals for each of the cancers, each of the immune checkpoint therapies where queried using Drugs.com that provides high quality reporting of FDA approvals for each medication. To determine if there was a significant difference in the number of approvals between athero-similar and -dissimilar cancers, a Fisher's exact test was performed comparing the number of approvals to overall possible approvals.

In-silico drug screening to identify putative therapeutic compounds

To predict the ability of individual compounds to reverse the detrimental gene signature and therefore identify putative therapeutics for cancer and atherosclerosis, a modified version of the OCTAD algorithm[24] was utilized. This calculates a reverse gene expression score (RGES), a measure of how well each compound reverses the detrimental gene signature and promotes the beneficial gene signature for each dataset. Specifically, it incorporates the Library of Integrated Network-Based Cellular Signatures (LINCS) dataset,[48] a library of disturbance expression profiles for 71 cell lines treated with 12,442 compounds. To improve the predictions, only cell lines corresponding to the cancer type of interest or hematopoietic cell lines (the best approximation for atherosclerosis) were taken into consideration. The RGES was defined as the

difference between two distribution similarity statistics (the Kolmogorov-Smirnov (KS) statistics). The first distribution included changes in detrimental genes and the second included changes in the beneficial genes. Therefore, the ideal scenario would be that all the detrimental genes were inhibited by the compound (i.e., all detrimental genes clustered to one tail of the drug distribution expression profiles [KS → −1]) and all the beneficial genes were upregulated (i.e., clustered to the opposite side of the distribution expression profile [KS → 1]), making the ideal final RGES value −2. A permutation procedure was used to estimate an empirical P-value by randomly permutating the detrimental and beneficial gene list 10,000 times.

QUANTIFICATION AND STATISTICAL ANALYSIS

As described in the methods details section above, multivariate cox regression was utilized to correlate transcriptomic data with patient information (i.e., survival, disease severity, etc.). The normalized enrichment score (NES) output from GSEA was used to quantify the impact of each individual pathway. For the clustering analysis in Figure 2B, the shared nearest neighbor clustering algorithm was used. The mean immune cell infiltration for each group of cancers was compared via t-test. Fisher's exact test was used to compare the number of FDA approvals for ICI between athero-similar and -dissimilar. For the drug prediction analyses, the reverse gene expression score was defined as the difference between two distribution similarity statistics (the Kolmogorov-Smirnov statistics) and a permutation procedure was used to estimate an empirical P-value by randomly permutating the detrimental and beneficial gene list 10,000 times.